

# The Influence of Molybdenum on the $\gamma'$ Phase in Experimental Nickel-Base Superalloys

W. T. LOOMIS, J. W. FREEMAN, AND D. L. SPONSELLER

The influence of 1, 3, and 5 at. pct Mo on the  $\gamma'$  precipitate has been studied in experimental wrought nickel-base superalloys containing about 14 at. pct Cr and  $6\frac{1}{2}$ , 9, or 12 at. pct Al, or 2 at. pct Al plus 4 at. pct Ti. Concentrations of all other elements were quite low to limit the observed effects to those of molybdenum alone. Molybdenum markedly increases the  $\gamma'$  solvus temperature, as determined by the sensitive and relatively simple technique of differential thermal analysis; correspondingly, the weight fraction of  $\gamma'$  increases with molybdenum additions for a given aging treatment. Molybdenum dissolves extensively in the  $\gamma'$  of the titanium-free alloys, but it dissolves to a considerably smaller extent in the  $\gamma'$  of the titanium-bearing alloys. Molybdenum substitutes for chromium in  $\gamma'$ , but does not alter the aluminum or titanium contents of this phase. Lattice parameters of both the matrix and the  $\gamma'$  are increased markedly by molybdenum, in proportion to the molybdenum contents of these phases. The resulting effects on lattice-parameter mismatch correlate rather well with observed  $\gamma'$  morphology, which tends to change from spheroidal to cuboidal in titanium-free alloys, and from cuboidal to spheroidal in 2 at. pct Al-4 at. pct Ti alloys, as molybdenum is added to these alloys.

**M**OST commercial nickel-base superalloys in use today depend primarily on a uniform dispersion of very fine particles of the  $\gamma'$  (gamma prime) phase for achieving suitable elevated-temperature strength. This phase has an ordered structure of the  $L1_2$  type, based on the formula  $Ni_3Al$ . Refractory metals contribute significantly to the outstanding strength of these superalloys at elevated temperatures, but relatively little effort has been devoted to delineating the fundamental effects of refractory elements on the characteristics of  $\gamma'$ . Guard and coworkers have reported limited solubility of molybdenum in the  $\gamma'$  of Ni-Al-Mo alloys at about 2150°F (1175°C).<sup>1,2</sup> Only recently has moderate solubility of refractory elements in the  $\gamma'$  of commercial nickel-base superalloys,<sup>3,4</sup> and the effects of molybdenum<sup>5</sup> and tungsten<sup>6</sup> on lattice parameter and on morphology of  $\gamma'$  in Ni-Cr-Al-Ti alloys, been reported. Because increased sophistication of modern alloy design, employing techniques such as the "PHACOMP"<sup>7</sup> analysis, has shown the need for basic information regarding the  $\gamma'$  phase, this investigation was undertaken to study the interaction of molybdenum with the  $\gamma'$  phase in nickel-base superalloys. The effects of this element on the  $\gamma'$  solvus temperature, and on the quantity, composition, lattice parameter, and morphology of  $\gamma'$  were studied in a systematic series of alloys.

## EXPERIMENTAL PROCEDURE

This study was conducted on four series of experimental wrought alloys of different "hardener" (Al + Ti) levels, the molybdenum content varying regularly within each series. Briefly stated, the influence of molybdenum on the  $\gamma'$  phase was determined by measuring the  $\gamma'$  solvus temperatures of the alloys, and by determining the weight fraction, composition, lattice parameter, and morphology of  $\gamma'$  precipitate for each alloy after prolonged aging at 1400°F (760°C) or 1700°F (927°C). Experimental techniques were described in detail by Loomis<sup>8</sup> and are only outlined in this section.

Sixteen alloys, the compositions of which are listed in Table I, were studied. Alloys were rather simple in composition, representing molybdenum additions to the Ni-Cr-Al system (Alloys 1 to 12) or the Ni-Cr-Ti-Al system (Alloys 13 to 16). These ternary and quaternary systems were chosen in preference to complex commercial alloys as the basis for this study in order to limit the observed effects to those of molybdenum alone. The existence of phase diagrams for these systems was an added advantage.<sup>9-13</sup> Carbon was purposely maintained at low levels in order to avoid any influence of structure- and time-dependent carbide reactions on the  $\gamma'$  phase. "Hardener" levels were approximately  $6\frac{1}{2}$ , 9, and 12 at. pct Al and 2 at. pct Al + 4 at. pct Ti. Molybdenum levels of approximately 0, 1, 3, and 5 at. pct were studied at each hardener level. The alloys were designed to have a fixed Ni/Cr ratio, about 5.2 based on analyzed concentrations in atomic percent.

Alloys were produced by vacuum-induction melting electrolytic nickel (99.95 pct), electrolytic chromium (99.48 pct), sintered molybdenum pellets (99.9 pct), aluminum ingot (99.5 pct), and titanium sponge (99.3 pct). A small quantity of graphite was added in the initial charge to deoxidize the melt by means of a carbon

W. T. LOOMIS is President, Logic Associates, Inc., Hanover, N. H. J. W. FREEMAN was formerly Professor of Metallurgical Engineering, University of Michigan, Ann Arbor, Mich. (Deceased, November, 1970). D. L. SPONSELLER is Metallurgical Research Supervisor, Climax Molybdenum Company of Michigan, Ann Arbor, Mich. This paper is based upon a thesis submitted by W. T. LOOMIS in partial fulfillment of the requirements for the degree of Doctor of Philosophy at the Horace H. Rackham School of Graduate Studies, The University of Michigan. Manuscript submitted June 28, 1971.

Table I. Chemical Composition of the Alloys\*

Alloy Number	Al	Ti	Mo	Cr	Ni
Weight Percent					
1	3.14	—†	—	14.22	82.53
2	3.10	—	2.05	13.87	80.87
3	3.09	—	5.25	13.38	78.17
4	3.15	—	8.61	12.88	75.25
5	4.37	—	—	14.29	81.23
6	4.32	—	2.05	13.93	79.59
7	4.32	—	5.09	13.41	77.07
8	4.32	—	8.14	12.90	74.54
9	5.80	—	—	13.53	80.56
10	5.83	—	2.03	13.32	78.71
11	5.95	—	4.95	12.86	76.13
12	5.87	—	7.70	12.56	73.76
13	1.05	3.49	—	13.94	81.41
14	1.04	3.43	2.00	13.63	79.79
15	1.04	3.40	4.93	13.17	77.35
16	1.02	3.40	7.96	12.70	74.81
Atomic Percent					
1	6.47	—	—	15.19	78.12
2	6.44	—	1.20	14.95	77.21
3	6.50	—	3.11	14.60	75.57
4	6.71	—	5.16	14.24	73.69
5	8.88	—	—	15.06	75.86
6	8.85	—	1.18	14.81	74.97
7	8.96	—	2.97	14.43	73.46
8	9.07	—	4.80	14.05	71.89
9	11.61	—	—	14.05	74.13
10	11.76	—	1.15	13.94	72.95
11	12.12	—	2.84	13.59	71.27
12	12.09	—	4.46	13.42	69.83
13	2.20	4.12	—	15.14	78.34
14	2.20	4.08	1.19	14.93	77.41
15	2.22	4.09	2.96	14.59	75.93
16	2.21	4.14	4.84	14.25	74.36

\*Aluminum was determined by atomic absorption analysis, titanium, molybdenum and chromium by gravimetric techniques and nickel by difference. The concentrations of trace elements are as follows, in wt pct: 0.004 to 0.011 C, 0.010 to 0.015 B, approx. 0.02 Si and 0.07 Fe

†Dash indicates not added and not analyzed.

boil prior to the addition of aluminum. Boron, included in each alloy in an analyzed concentration of 0.010 to 0.015 pct to enhance hot-workability, was added as NiB. Alloys at each "hardener" level were melted in Al<sub>2</sub>O<sub>3</sub> crucibles as a single heat, with each heat being split into four 10 lb. (4.5 kg) ingots containing approximately 0, 1, 3, and 5 at. pct Mo, respectively.

The 2.5 in. (64 mm) diam ingots were converted to bars slightly less than  $\frac{3}{4}$  in. (19 mm) square in a thermomechanical sequence that was designed to eliminate any serious microsegregation and to avoid an excessively large grain size. The alloys were held at 2250°F (1232°C), a total time of approximately 12 hr, during preliminary and intermediate homogenization treatments and during the actual rolling process.

The influence of molybdenum on the  $\gamma'$  solution temperature was determined on specimens that had been held at 1800°F (982°C) for 1 hr and furnace-cooled to develop the maximum amount of  $\gamma'$  precipitate. Specimens  $\frac{5}{16}$  in. (8 mm) in diameter by  $\frac{5}{8}$  in. (16 mm) in length were then subjected to differential thermal analysis (DTA), a technique in which the temperature difference between the test specimen and a nickel reference specimen was measured while both were heated

and cooled in argon at a rate of about 18°F/min (10°C/min). Abrupt changes were observed in the trace of the temperature-difference curve, providing clear indications of the  $\gamma'$  solvus temperature during heating and cooling. This is thought to be the first measurement of  $\gamma'$  solvus temperature by differential thermal analysis.

Specimens for all studies other than DTA were aged at 1400°F (760°C) for 63, 328, or 1000 hr, and at 1700°F (927°C) for 3, 27, or 112 hr, followed by a vigorous quench in cold water. Although metallographic and some X-ray diffraction studies were performed on solid samples, the major research effort was performed on  $\gamma'$  precipitate extracted from specimens aged the maximum time at each temperature. The extracts were obtained electrolytically with a solution of 15 pct phosphoric acid in water. The weight fraction of  $\gamma'$  was determined by weighing the extracted  $\gamma'$  and comparing this weight with the overall weight loss of the specimen. The chemical composition of the extracted  $\gamma'$  was determined by atomic absorption analysis and by electron microprobe analysis. Agreement between the two methods was good, but the atomic absorption results are reported here because they exhibited considerably less scatter. Lattice parameter measurements on solid samples and extracted  $\gamma'$  were made with a carefully aligned diffractometer, employing nickel-filtered copper radiation. Lattice parameters were computed by a least-squares method.

## RESULTS AND DISCUSSION

### $\gamma'$ Solvus Temperature

The influence of molybdenum on the  $\gamma'$  solvus temperature was determined from differential thermal analysis curves, as represented by the schematic diagram shown in Fig. 1. As seen from this diagram, the  $\gamma'$  solvus temperature during heating is the temperature at which the  $\Delta T$  curve returns to the base line after being depressed by the endothermic dissolution of  $\gamma'$ .

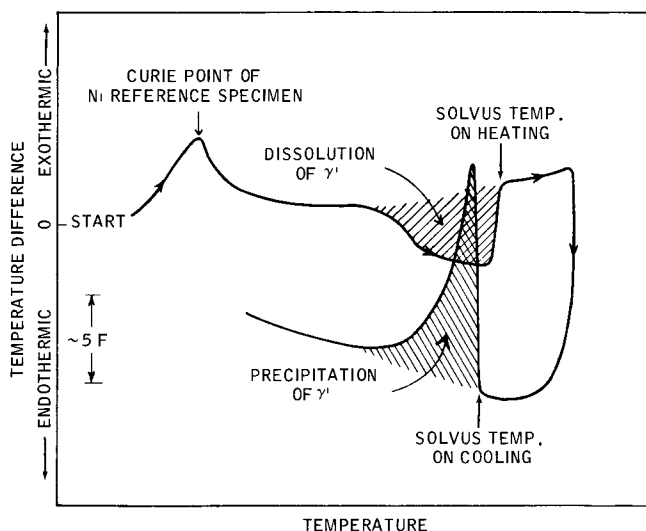


Fig. 1—Schematic representation of a differential thermal analysis trace, obtained at a heating and cooling rate of approximately 18°F/min (10°C/min).

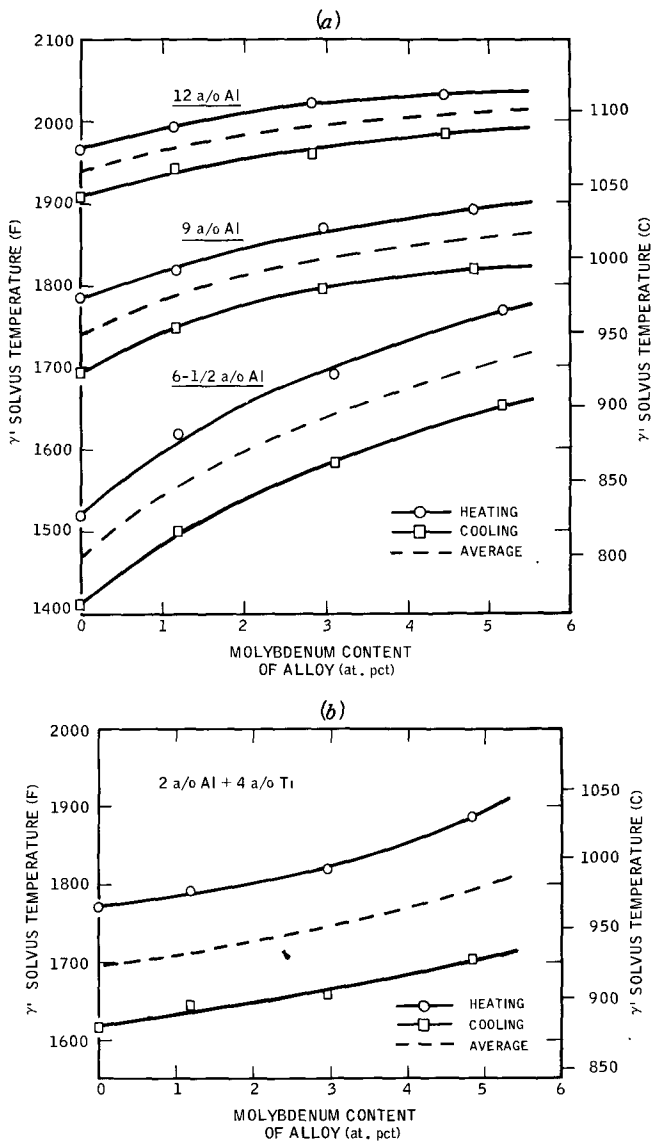


Fig. 2—Influence of molybdenum on  $\gamma'$  solvus temperature.

During cooling, the  $\gamma'$  solvus temperature is indicated by the point where the curve sharply rises from the base line, as a result of the exothermic precipitation of  $\gamma'$ . The DTA results are related to molybdenum concentration in Fig. 2. Here, each series of alloys is represented by a band, the upper solid curve in each band denoting solvus temperatures measured during heating, and the lower solid curve representing those measured during cooling. The noncoincidence of the heating and cooling curves precludes the reporting of an equilibrium solvus curve for each series of alloys. In estimating the location of the equilibrium curve, the cooling curve might be expected to lie considerably farther from the equilibrium curve than does the heating curve, because of the undercooling normally associated with precipitation processes. The results of recent experiments,<sup>14</sup> however, which show that the  $\gamma'$  solvus temperature measured during heating declines significantly as heating rate is reduced from the 18°F/min (10°C/min) rate of this study, indicate that the heating curve for each series of alloys also is dis-

placed by at least a moderate distance from the equilibrium curve. For this reason, the center of the band, represented by a dashed curve, may be taken as a first approximation to the equilibrium  $\gamma'$  solvus curve for each series of alloys. In Fig. 2(a), the difference between solvus temperatures measured on heating vs cooling for the Ni-Cr-Al-Mo alloys tends to become smaller as the aluminum content increases from 6½ to 12 at. pct Al, probably because of faster diffusion at the higher solvus temperatures of the higher-aluminum alloys. Molybdenum raises the  $\gamma'$  solvus temperature monotonically at each aluminum level, the increase at 5 at. pct molybdenum being approximately 240°F (133°C) in the 6½ at. pct Al series, 120°F (67°C) in the 9 at. pct Al series, and approximately 75°F (42°C) in the 12 at. pct Al series. The DTA results for the Ni-Cr-Ti-Al-Mo alloys, Fig. 2(b), exhibit a wider separation between the heating and cooling curves than for the Ni-Cr-Al-Mo alloys, presumably because of slow diffusion of the large titanium atoms. These results show that the  $\gamma'$  solvus band rises continuously as molybdenum is added in this high-titanium series of alloys. Molybdenum raises  $\gamma'$  solvus temperature by a smaller amount, approximately 100°F (56°C), in this series of alloys, however, than in the two titanium-free series having the most nearly comparable ranges of solvus temperatures (the 6½ and 9 at. pct Al alloys).

As a means of describing the influence of molybdenum on the  $\gamma'$  solvus surface, *i. e.*, on the boundary between the  $\gamma$  and the  $\gamma + \gamma'$  fields, in the Ni-Cr-Al-temperature phase model, the foregoing results are plotted against aluminum content in Fig. 3. For each alloy, the average of the values obtained during heating and cooling is plotted in Fig. 3. These mean values are thought to provide a reasonably good representation of the equilibrium  $\gamma'$  solvus boundary in the Ni-Cr-Al system, and the effects of molybdenum thereon. Molybdenum is seen to shift the boundary upward markedly, the increase being greatest at lower aluminum contents.

The  $\gamma'$  solvus temperatures for the titanium-bearing alloys are also shown in Fig. 3. In addition to illustrating the effect of molybdenum on the  $\gamma'$  solvus temperature in this series of alloys, these data points indicate that, on an atomic basis, titanium is more effective than aluminum in raising  $\gamma'$  solvus temperature, inasmuch as these points lie above the curves for the titanium-free alloys.

#### Weight Fraction of $\gamma'$

As described in the previous section, the  $\gamma'$  solvus curve in the Ni-Cr-Al system represented by Fig. 3 is raised by molybdenum additions to the system. Alternatively, the curves of Fig. 3 show that, at any temperature, molybdenum reduces aluminum solubility in the  $\gamma$  matrix. This suggests that molybdenum additions should increase the quantity of  $\gamma'$  at any temperature, a supposition that is borne out by studies of specimens aged for 1000 hr at 1400°F (760°C) or 112 hr at 1700°F (927°C). In these studies, the weight percent of  $\gamma'$  extracted electrolytically from the aged specimens was determined. The results, shown in Fig. 4, indicate that the weight fraction of  $\gamma'$  is affected by molybdenum. For the Ni-Cr-Al-Mo alloys aged at 1400°F (760°C),

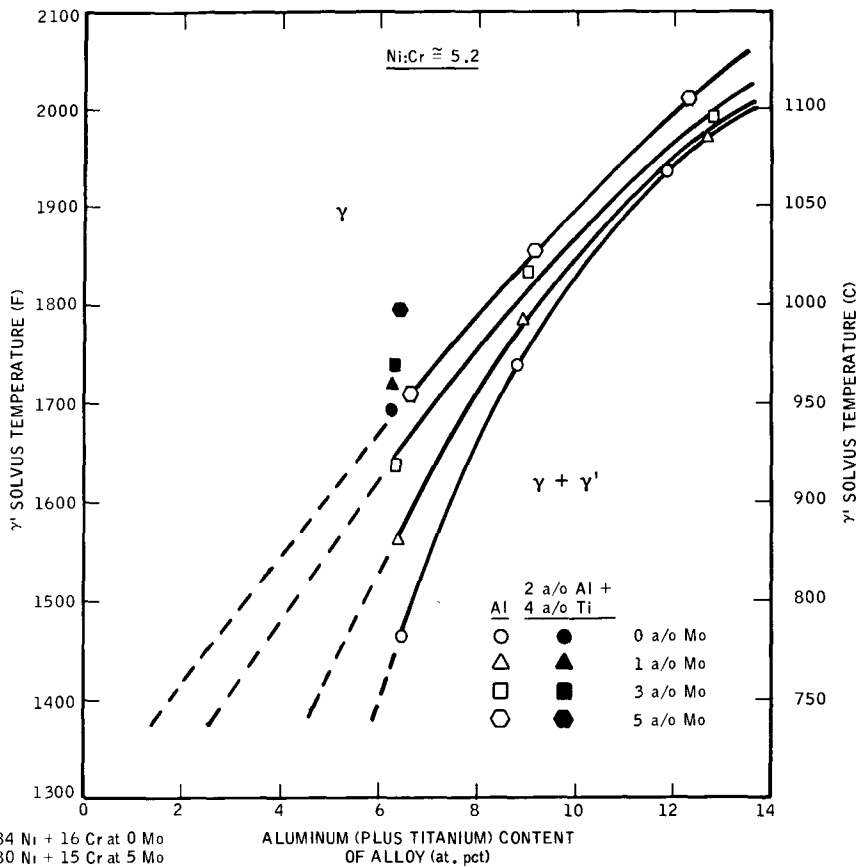


Fig. 3—Influence of molybdenum on  $\gamma'$  solvus curve of Ni-Cr-Al system, for alloys with a Ni:Cr ratio of approximately 5.2. Data points for the titanium-bearing alloys are also shown.

Fig. 4(a), the weight fraction rises continuously with increasing molybdenum content at all three aluminum levels. The results for the specimens aged at 1700°F (927°C) show that molybdenum causes a similar continuous increase in  $\gamma'$  weight fraction at the 9 at. pct

Al level, and a strong initial increase at 1 and 3 at. pct Mo, followed by a leveling off at the highest molybdenum concentration in the 12 at. pct Al alloys, Fig. 4(b). The 1700°F (927°C) curve cannot be drawn for the 6½ at. pct Al alloys because of the absence of  $\gamma'$  due to

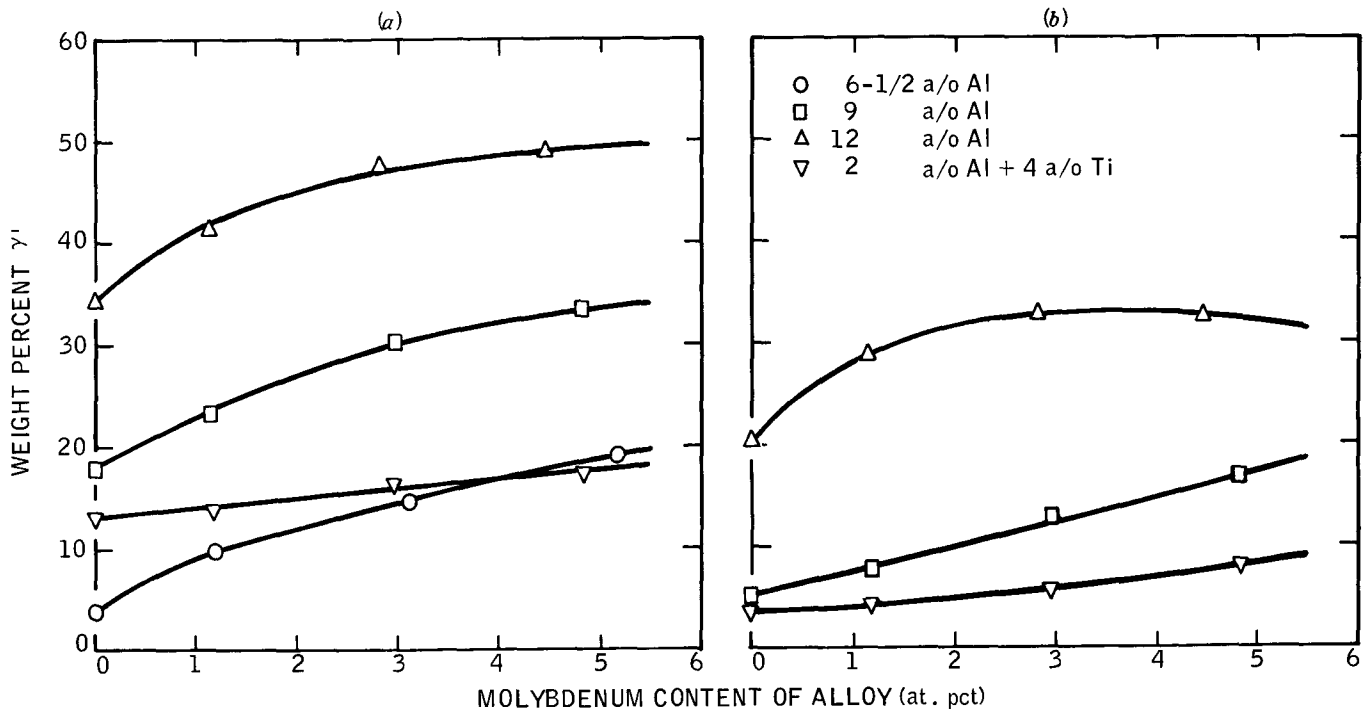


Fig. 4—Influence of molybdenum on weight fraction of  $\gamma'$  extracted from specimens aged at (a) 1400°F (760°C) for 1000 hr, or (b) 1700°F (927°C) for 112 hr.

Table II. Chemical Composition of the Extracted  $\gamma'$  Phase

Alloy Number	Heat Treatment Prior to Extraction							
	Aged for 1000 Hr at 1400°F (760°C)				Aged for 112 Hr at 1700°F (927°C)			
	Mo	Cr	Al	Ti	Mo	Cr	Al	Ti
	Weight Percent							
1	0	7.1	8.4	—	—	—	—	—
2	3.3	4.2	8.2	—	—	—	—	—
3	5.6	4.1	8.3	—	—	—	—	—
4	6.5	3.5	8.1	—	—	—	—	—
5	0	7.5	8.5	—	0	8.5	10.0	—
6	2.6	5.5	8.2	—	1.8	7.0	9.1	—
7	5.0	4.2	8.5	—	3.9	5.1	8.1	—
8	6.6	3.1	8.2	—	5.5	4.0	8.1	—
9	0	6.9	8.2	—	0	7.6	8.6	—
10	2.4	4.6	8.0	—	2.1	6.0	8.5	—
11	4.7	2.8	8.6	—	4.5	4.5	8.2	—
12	6.5	4.4	8.1	—	5.8	4.2	8.5	—
13	0	2.1	3.8	12.1	0	2.0	3.7	11.5
14	0.7	1.9	3.6	12.6	0.5	2.1	3.8	11.6
15	1.1	1.2	3.6	10.8	1.0	1.5	4.1	13.1
16	1.6	1.1	3.7	11.1	1.4	1.1	4.2	11.8
	Atomic Percent							
1	0	7.2	16.5	—	—	—	—	—
2	1.8	4.3	16.4	—	—	—	—	—
3	3.2	4.3	16.7	—	—	—	—	—
4	3.7	3.7	16.4	—	—	—	—	—
5	0	7.6	16.7	—	0	8.5	19.3	—
6	1.5	5.7	16.3	—	1.0	7.1	17.8	—
7	2.8	4.4	17.0	—	2.2	5.3	16.2	—
8	3.7	3.3	16.6	—	3.1	4.2	16.3	—
9	0	7.0	16.2	—	0	7.7	16.8	—
10	1.3	4.8	16.0	—	1.2	6.2	16.8	—
11	2.6	2.9	17.3	—	2.5	4.7	16.4	—
12	3.7	4.6	16.4	—	3.3	4.4	17.1	—
13	0	2.2	7.8	13.8	0	2.1	7.5	13.1
14	0.39	2.0	7.3	14.4	0.28	2.2	7.7	13.3
15	0.63	1.3	7.5	12.4	0.57	1.6	8.4	14.9
16	0.92	1.2	7.6	12.8	0.79	1.1	8.6	13.5

the lower solvus temperatures. The curves for the titanium-bearing alloys corresponding to these two aging temperatures also show that molybdenum causes continuous increases in weight fraction of  $\gamma'$ . These increases are smaller than for titanium-free alloys.

Any study of extracted precipitate carries with it the possibility that the precipitate will be contaminated or partially dissolved during the extraction process. Electron metallographic examination of extracted particles failed to reveal either contamination by the extracting solution or any obvious rounding of the edges of cuboidal particles. The authors recognize, however, the possibility of partial dissolution of  $\gamma'$  particles. Subsequent to the preparation of the extract for this investigation, Krieger and others<sup>4,15</sup> reported that other electrolytes including aqueous solutions of ammonium phosphate plus tartaric acid and ammonium sulfate plus citric acid may yield greater quantities of  $\gamma'$  than those obtained with the 15 pct phosphoric acid electrolyte used in this investigation. In a study of  $\gamma'$  coalescence, Biss<sup>16</sup> has recently measured volume fractions of  $\gamma'$  in some of the same aged specimens described in Fig. 4. Studying those specimens that lend themselves to measurement by electron metallography, *i. e.*, specimens with low volume fractions and/or large particles of  $\gamma'$ , he observed significantly

larger quantities of  $\gamma'$  than those shown in Fig. 4, even after allowing for the density-related differences between volume and weight fractions. This supports the findings of Krieger and coworkers<sup>4,15</sup> about the possible dissolution of  $\gamma'$  during electrolytic extraction. The effect of molybdenum on volume fraction of  $\gamma'$ , however, was found by Biss to be approximately the same as its effect on weight fraction shown in Fig. 4. Although the data plotted in Fig. 4 may be affected somewhat by partial dissolution of  $\gamma'$ , the curves of Fig. 4 are therefore thought to represent the influence of molybdenum on the quantity of  $\gamma'$  with reasonable accuracy.

#### Chemical Composition of $\gamma'$

The chemical compositions of  $\gamma'$  precipitate extracted from specimens aged at 1400° and 1700°F (760° and 927°C) are presented in Table II. These results are plotted as a function of the molybdenum content of the alloys in Figs. 5 through 8. In each of these graphs, the results for all the Ni-Cr-Al-Mo alloys are represented by a single curve at each temperature, since there is little difference in  $\gamma'$  composition for the three aluminum levels.

Significant concentrations of molybdenum were found in the  $\gamma'$  of all molybdenum-containing alloys, Fig. 5. For each series of alloys, the concentration of molybdenum in the  $\gamma'$  increases continuously as molybdenum is added to the base alloy. In the Ni-Cr-Al-Mo alloys, molybdenum dissolves quite extensively in  $\gamma'$ , the maximum concentration being 3.7 at. pct Mo. Substitution of titanium for most of the aluminum, however, restricts molybdenum contents of the  $\gamma'$  to much lower levels, the maximum value in these high-titanium alloys being 0.92 at. pct Mo.

The dotted lines in Fig. 5 represent equal partition of molybdenum between the matrix and  $\gamma'$  phases. It is evident from Fig. 5(a) that, for the Ni-Cr-Al-Mo alloys aged 1000 hr at 1400°F (760°C), molybdenum actually dissolves preferentially in the  $\gamma'$  phase at the 1 at. pct Mo level. As molybdenum content of the alloy increases beyond approximately 2.5 at. pct, however, molybdenum partitions preferentially into the matrix phase. Results for these alloys aged 112 hr at 1700°F (927°C), Fig. 5(b), show that molybdenum partitions equally between  $\gamma'$  and the matrix in the 1 at. pct Mo alloys, and in favor of the matrix with further increases in the molybdenum concentration of the alloy.

The molybdenum concentrations in the  $\gamma'$  decrease a small amount as the aging temperature increases from 1400°F (760°C) to 1700°F (927°C) in all four series of alloys. This may explain why Guard *et al.* reported little molybdenum solubility in Ni<sub>3</sub>Al at a much higher temperature, 2150°F (1175°C).<sup>1,2</sup> More recently, however, Maxwell attained a molybdenum concentration of 4 wt pct (2.5 at. pct) in Ni<sub>3</sub>Al by means of a diffusion couple of Ni<sub>3</sub>Al and Ni<sub>3</sub>Mo held for 100 hr at 2200°F (1204°C).<sup>17</sup>

As noted above, molybdenum solubility in  $\gamma'$  is reduced sharply by titanium. This is consistent with the results of a study reported by Krieger and Baris of  $\gamma'$  extracted from commercial nickel-base superalloys having a wide range of compositions.<sup>4</sup> An analysis of their data shows that molybdenum tends to partition away from the  $\gamma'$  and into the matrix as the Ti/Al ratio increases.

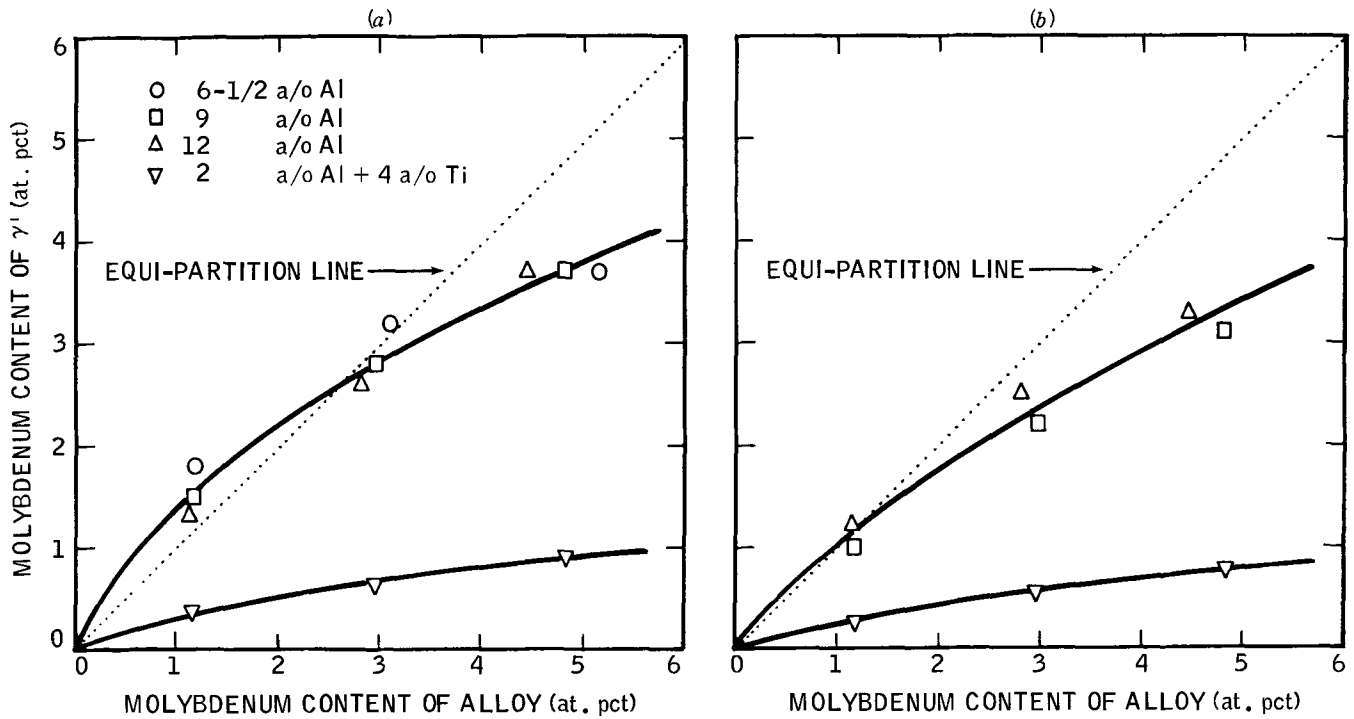


Fig. 5—Influence of the molybdenum content of the alloy on the molybdenum content of  $\gamma'$  precipitate extracted from specimens aged at (a) 1400°F (760°C) for 1000 hr, or (b) 1700°F (927°C) for 112 hr.

Molybdenum lowers the chromium content of  $\gamma'$  appreciably, Fig. 6. In the Ni-Cr-Al-Mo alloys, the effect is especially pronounced for molybdenum additions ranging up to 3 at. pct. The curves for the titanium-bearing alloys in Fig. 6 are displaced markedly downward from those for the aluminum alloys. This reflects the drastic influence of titanium on chromium solu-

bility in  $\gamma'$ , as described by Taylor for the Ni-Cr-Al-Ti system.<sup>13</sup> Nevertheless, molybdenum also lowers the chromium content of the  $\gamma'$  in the titanium-bearing alloys.

Figs. 7 and 8 show the influence of molybdenum on the aluminum and titanium concentrations, respectively, of  $\gamma'$ . In these plots, data for both aging tem-

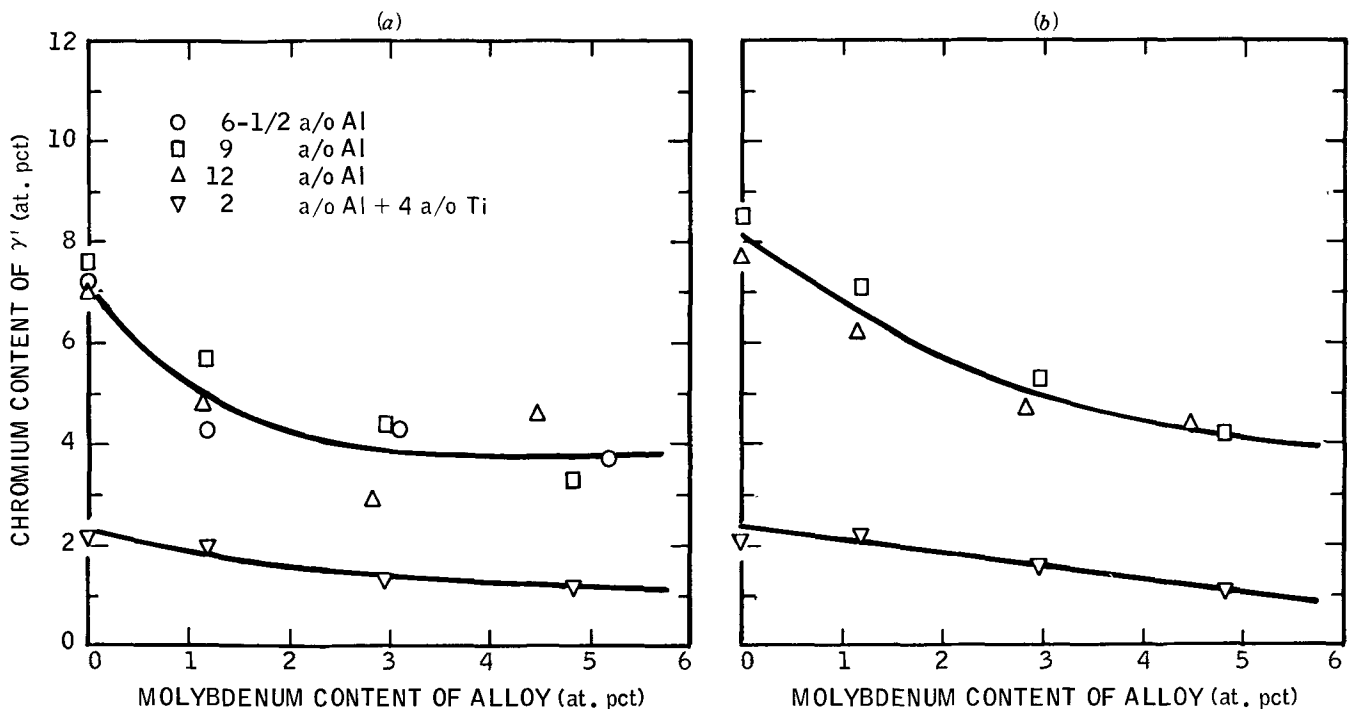


Fig. 6—Influence of the molybdenum content of the alloy on the chromium content of  $\gamma'$  precipitate extracted from specimens aged at (a) 1400°F (760°C) for 1000 hr, or (b) 1700°F (927°C) for 112 hr.

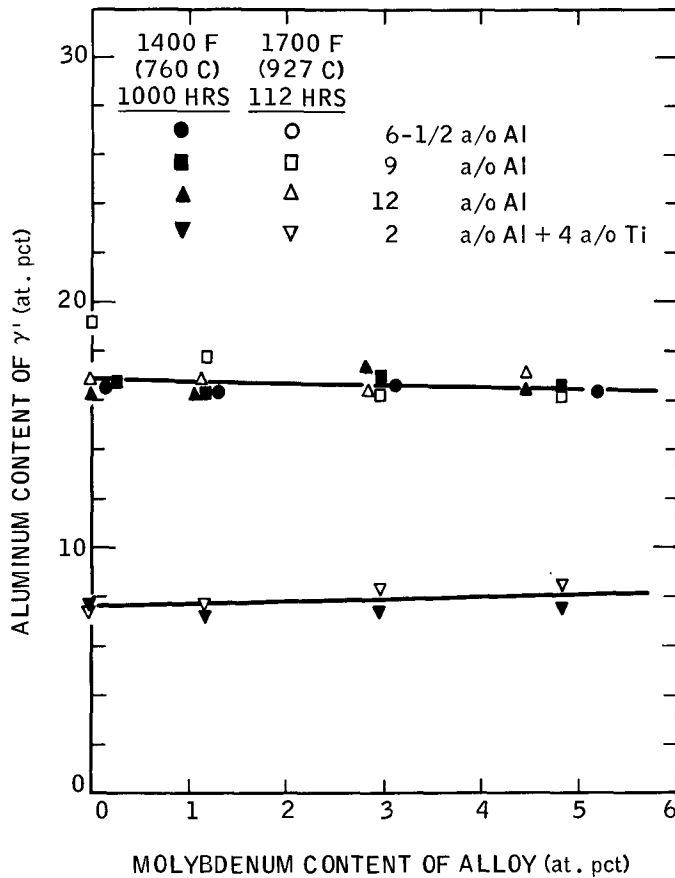


Fig. 7—Influence of the molybdenum content of the alloy on the aluminum content of  $\gamma'$  precipitate extracted from specimens aged at 1400° F (760°C) for 1000 hr or 1700° F (927°C) for 112 hr.

peratures are represented by single curves for each of these solutes. Molybdenum is seen to have no significant effect on the aluminum content of the  $\gamma'$ . As in the case of chromium, the large downward displace-

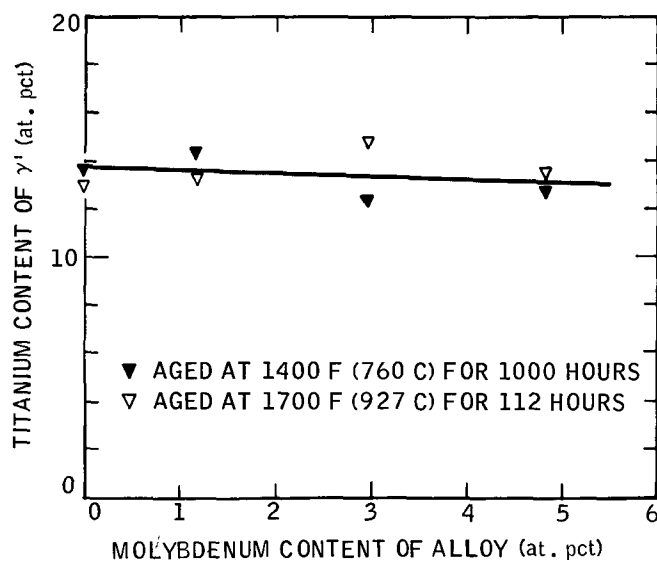


Fig. 8—Influence of the molybdenum content of the alloy on the titanium content of  $\gamma'$  precipitate extracted from specimens aged at 1400° F (760°C) for 1000 hr or 1700° F (927°C) for 112 hr.

ment of the curve for aluminum content associated with the addition of titanium is consistent with the results of Taylor's study of the Ni-Cr-Al-Ti system.<sup>13</sup> It is worthy of note that the average Al/Ti ratio (on an atomic basis) in the  $\gamma'$  of the present alloys is nearly the same as the average Al/Ti ratio of the alloys, 0.58 vs 0.54. This agrees with the findings of Kriege and Baris for commercial alloys.<sup>4</sup>

The chemical makeup of  $\gamma'$  is summarized in the bar graphs of Fig. 9. This type of graphical representation of the composition data illustrates several important points. First, the sum of molybdenum plus chromium concentrations is essentially constant for each series of alloys at both aging temperatures as molybdenum content of the alloy increases, showing that molybdenum substitutes chemically for chromium in  $\gamma'$ . Second, the chromium plus molybdenum content of the  $\gamma'$  is reduced sharply by the substitution of titanium for a major part of the aluminum in these alloys. Because this implies a rejection of these Group VI-A elements to the matrix, this could help explain why titanium has been reported by Dreshfield and Ashbrook<sup>18</sup> to promote  $\sigma$  formation in the nickel-base superalloy, IN-100. Finally, the sum of the Mo, Cr, Al, and Ti concentrations in Fig. 9 equals approximately 25 at. pct, suggesting (but not proving) that these atoms occupy corner sites in the  $\gamma'$  unit cell. The nickel concentration of approximately 75 at. pct (by difference), which agrees with the average concentration of 74 at. pct Ni (plus minor amounts of cobalt and iron) detected in the  $\gamma'$  of commercial alloys by Kriege and Baris,<sup>4</sup> corresponds to the occupation of the face-centered sites by nickel atoms. The close agreement of the present results with the formula  $Ni_3(Al, Ti, Cr, Mo)$  may be only fortuitous, since other investigators have claimed that chromium, or chromium and molybdenum atoms can occupy face-centered as well as corner sites.<sup>3,15,19,20</sup>

#### Lattice Parameter and Morphology

Lattice parameters of  $\gamma'$  extracted from specimens aged at 1400° and 1700° F (760° and 927°C) are listed in Table III. The results for specimens aged 1000 hr at 1400° F (760°C) and 112 hr at 1700° F (927°C) are plotted in Fig. 10. These graphs show that molybdenum causes significant and continuous increases in  $\gamma'$  lattice parameter. The increases are greatest for the Ni-Cr-Al-Mo alloys, and considerably smaller for the titanium-bearing alloys, in keeping with the greater molybdenum solubility in  $\gamma'$  in the former alloys. This influence of titanium on the expansion of the  $\gamma'$  lattice by molybdenum is consistent with results obtained on Ni-Cr-Al-Ti-Mo alloys by Maniar and Bridge<sup>21</sup> and Peter *et al.*<sup>5</sup> These investigators observed molybdenum to increase the  $\gamma'$  lattice parameter considerably less than in the titanium-free alloy of this study, but somewhat more than in the high-titanium alloys of this study. The molybdenum effect therefore increases with increasing Al/Ti ratio, in going from the titanium-bearing alloys of this study to those of Maniar and Bridge<sup>21</sup> and finally to those of Peter *et al.*<sup>5</sup>

The large upward displacement of the curves of  $\gamma'$  lattice parameter for the titanium-bearing alloys, relative to those for the titanium-free alloys in Figs. 10(a) and 10(b) reflects the presence of the large tita-

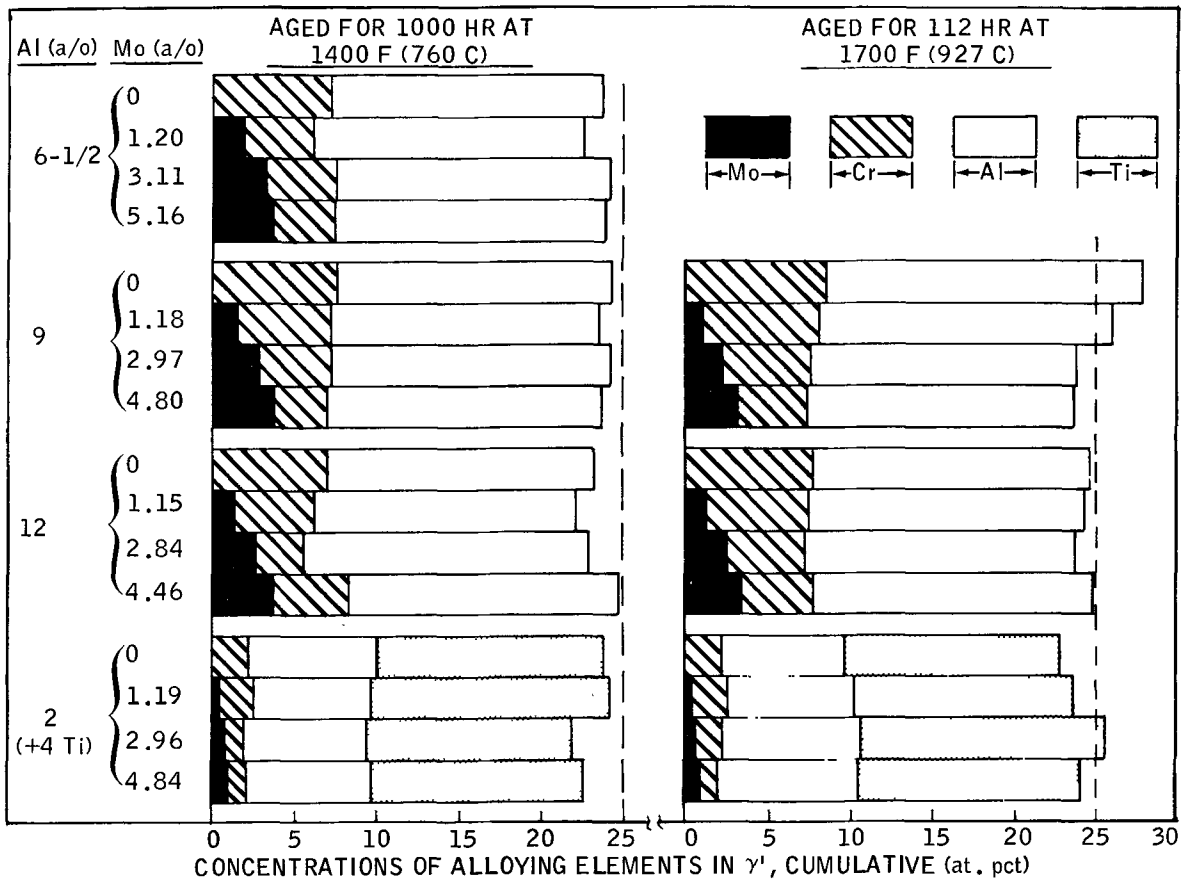


Fig. 9—Composition (bal Ni) of  $\gamma'$  shown as the sum of the individual concentrations of Mo, Cr, Al, and Ti in  $\gamma'$  precipitate extracted from specimens aged at 1400° F (760° C) for 1000 hr or 1700° F (927° C) for 112 hr.

nium atoms in the  $\gamma'$  of that series of alloys. This increase is consistent with the large increase in lattice parameter reported by Nordheim and Grant<sup>22</sup> after making a similar substitution of titanium for aluminum to produce a Ni-Cr-Al-Ti alloy.

Although the main research effort was expended on specimens aged for 1000 hr at 1400° F (760° C) or 112 hr

at 1700° F (927° C), a limited number of lattice parameters were determined for shorter aging times, Table III. The closeness of these parameters to the values for the maximum aging times (average difference = 0.0005 Å) suggests that the chemical composition of the  $\gamma'$  is essentially constant over the time intervals studied. Furthermore, it is worth noting that the lat-

Table III. Lattice Parameters of  $\gamma'$  and Matrix after Aging at 1400° and 1700° F (760° and 927° C), Å

Alloy Number	1400° F (760° C)					1700° F (927° C)				
	$\gamma'$				Matrix 1000 Hr	$\gamma'$				Matrix 112 Hr
	63 Hr Extracted	328 Hr Extracted	1000 Hr Extracted	<i>In Situ</i>		3 Hr Extracted	27 Hr Extracted	112 Hr Extracted	<i>In Situ</i>	
1	—*	—	3.5594	—	3.5537	—	—	—	—	—
2	—	—	3.5649	—	3.5596	—	—	—	—	—
3	—	—	3.5699	—	3.5669	—	—	—	—	—
4	—	—	3.5733	—	3.5779	—	—	—	—	—
5	3.5604	—	3.5601	—	3.5535	—	—	3.5614	—	3.5581
6	3.5653	3.5652	3.5651	—	3.5602	—	—	3.5655	—	3.5645
7	—	—	3.5701	—	3.5714	3.5701	3.5699	3.5695	—	3.5717
8	3.5722	—	3.5733	3.5742	3.5794	3.5741	—	3.5726	—	3.5816
9	—	—	3.5612	—	3.5619	—	—	3.5625	—	3.5609
10	—	—	3.5660	—	3.5670	—	—	3.5666	—	3.5674
11	—	—	3.5711	—	3.5765	—	—	3.5710	—	3.5779
12	—	—	3.5744	3.5766	(3.5865)*	—	—	3.5744	3.5773	3.5917
13	—	—	3.5895	—	3.5582	—	—	3.5885	—	3.5625
14	—	—	3.5902	3.5805	3.5629	—	—	3.5892	—	3.5679
15	3.5915	3.5914	3.5912	3.5816	3.5718	3.5903	3.5905	3.5902	—	3.5755
16	—	—	3.5923	—	3.5807	—	—	3.5915	—	3.5839

\*Not measured. The value shown in parentheses was determined by extrapolation of the values for alloys 9 to 11



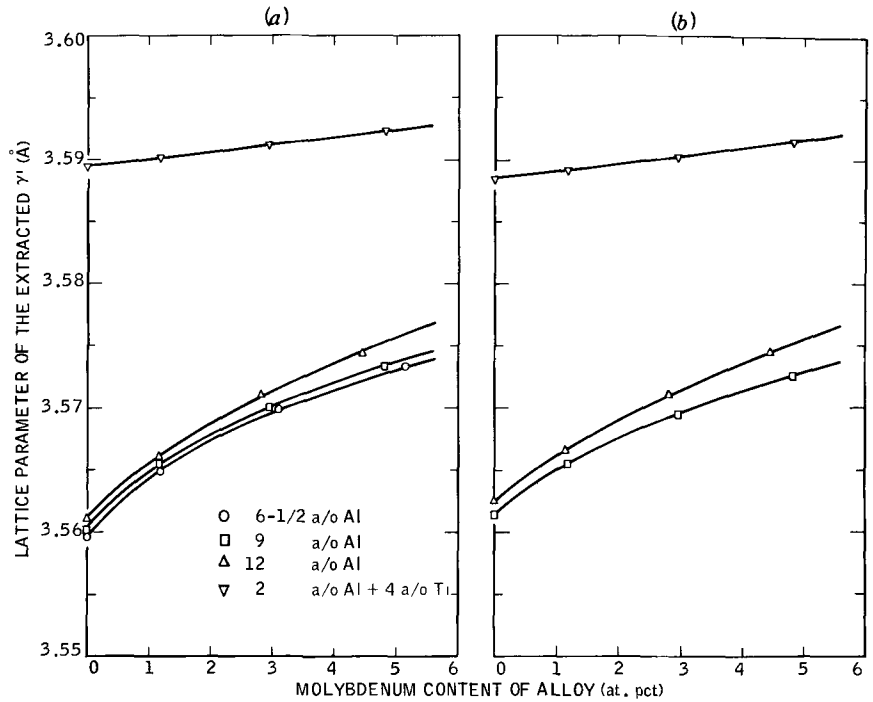


Fig. 10—Influence of the molybdenum content of the alloy on the lattice parameter of  $\gamma'$  precipitate extracted from specimens aged at (a) 1400°F (760°C) for 1000 hr, or (b) 1700°F (927°C) for 112 hr.

tice parameters of  $\gamma'$  are essentially the same at 1700°F (927°C) as at 1400°F (760°C), the average difference for an alloy being 0.0007Å or 0.02 pct. This is consistent with the similarity in composition of  $\gamma'$  between the two temperatures, noted earlier.

It has been possible to test the agreement between lattice parameter and chemical composition of the  $\gamma'$  by means of published data regarding expansion of the lattice of pure nickel by Al, Cr, Mo, and Ti in solid solution. Assuming simple additivity of the effects of individual elements, lattice parameters were calculated by means of the following equation, determined from published data.<sup>23</sup>

$$a_{\gamma'} = a_{\text{Ni}} + 0.00186 (\text{at. pct Al}) + 0.00105 (\text{at. pct Cr}) + 0.00435 (\text{at. pct Mo}) + 0.00337 (\text{at. pct Ti})$$

where  $a_{\gamma'}$  = calculated lattice parameter of the  $\gamma'$  in angstroms and  $a_{\text{Ni}} = 3.5240\text{Å}$ , the reported lattice parameter for nickel.<sup>23</sup> This equation ignores, of course, any effects related to the ordered structure of  $\gamma'$ . The coefficients in this equation indicate that, on an atomic basis, lattice parameter is increased slightly by chromium, moderately by aluminum, and strongly by titanium and molybdenum, the molybdenum effect being more than four times that of chromium. Fig. 11 shows that there is surprisingly good agreement between calculated and measured values, with all data points lying reasonably close to the dotted line that corresponds to perfect agreement. This provides a certain amount of confidence in the chemical compositions of the  $\gamma'$ , Table II, upon which the calculated lattice parameters are based. As seen from Fig. 11, the data points for the titanium-bearing alloys show a greater variation between calculated and measured values than for the titanium-free alloys, with titanium causing a larger expansion of the  $\gamma'$  lattice parameter than expected. Increasing the coefficient for titanium in the above equation by 12 pct, to 0.00378, causes

close agreement between calculated and measured values for the titanium-bearing alloys. This suggests that titanium has a somewhat greater influence on the lattice parameter of  $\gamma'$  than on that of pure nickel.

Because molybdenum exerts a strong influence on lattice parameter, and because in most of the aged specimens molybdenum dissolves more extensively in the matrix than in the  $\gamma'$ , the mismatch between the lattice parameters of these two phases changes significantly as molybdenum is added in each series of alloys. This should cause variations in  $\gamma'$  morphology in the

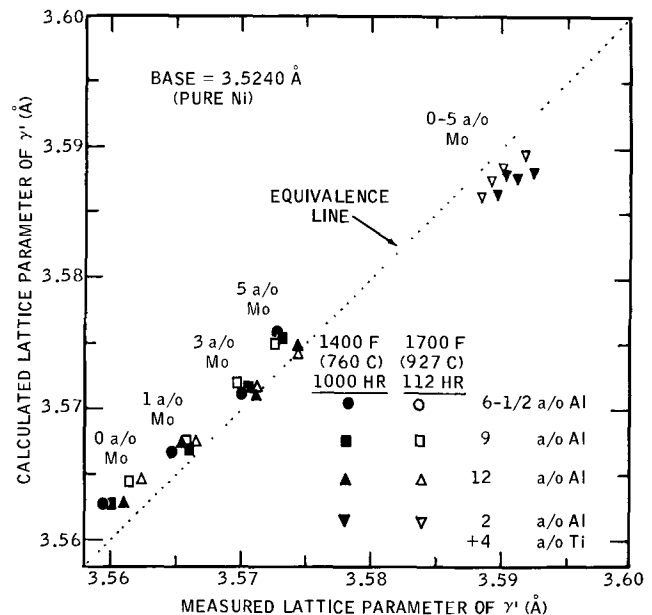


Fig. 11—Correlation of the  $\gamma'$  lattice parameter, calculated from the chemical composition of the  $\gamma'$ , with the measured  $\gamma'$  lattice parameter.

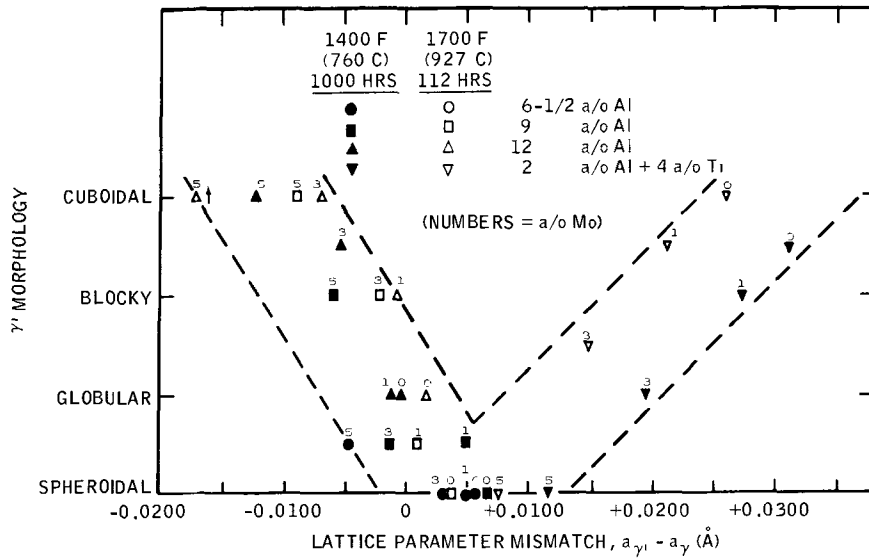


Fig. 12—Influence of lattice-parameter mismatch on the morphology of the  $\gamma'$  particles.

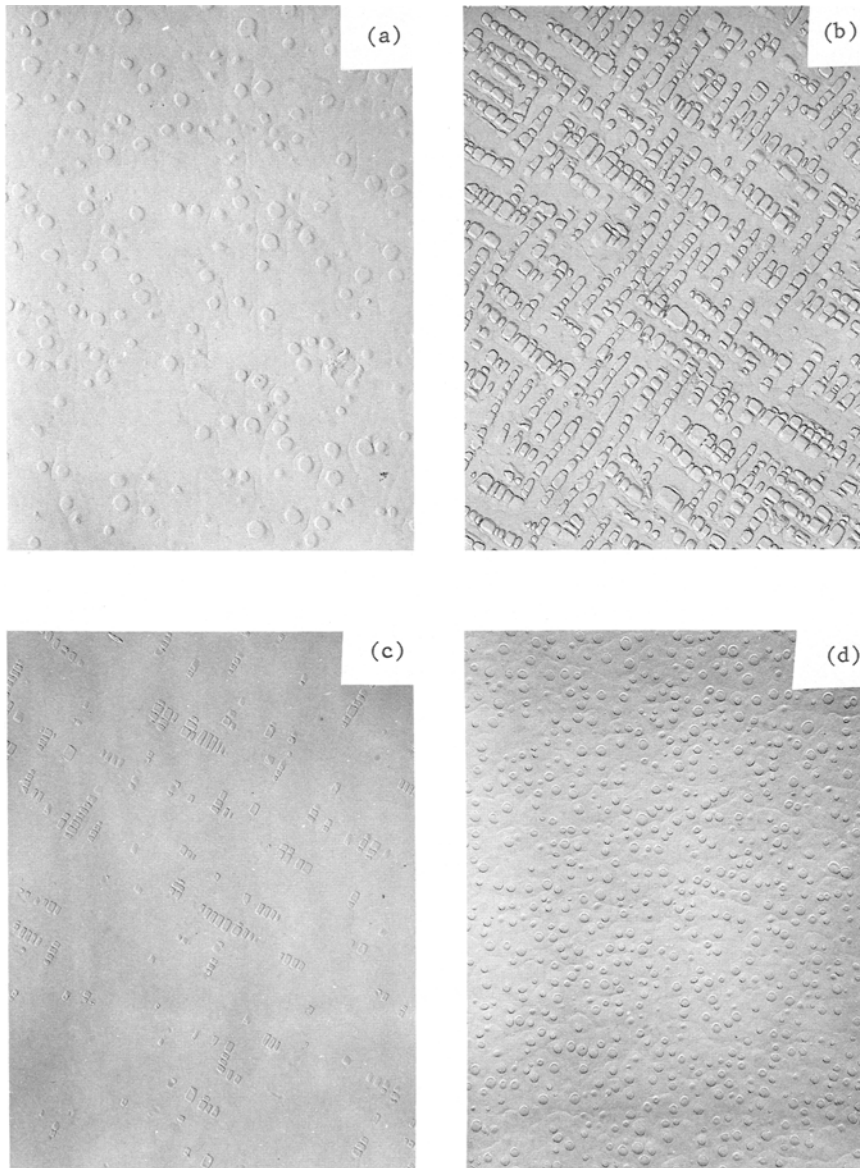


Fig. 13—Influence of molybdenum content and lattice-parameter mismatch ( $\alpha_{\gamma'} - \alpha_{\gamma}$ ) on the morphology of  $\gamma'$  particles after aging for 112 hr at 1700°F (927°C). Magnification 4150 times. (a) and (b)—Alloys containing 9 at. pct Al: (a) Alloy No. 5 (0 at. pct Mo),  $\Delta a = +0.0033\text{\AA}$ ; (b) Alloy No. 8 (4.80 at. pct Mo),  $\Delta a = -0.0090\text{\AA}$ . (c) and (d)—Alloys containing 2 at. pct Al + 4 at. pct Ti: (c) Alloy No. 13 (0 at. pct Mo),  $\Delta a = +0.0260\text{\AA}$ ; (d) Alloy No. 16 (4.84 at. pct Mo),  $\Delta a = +0.0076\text{\AA}$ .

present group of alloys. The results of earlier investigations<sup>24-26</sup> show that the  $\gamma'$  particles in nickel-base superalloys change from spheroids to cuboids (and ultimately to rods or plates) as lattice-parameter mismatch increases, because of the ability of the cubic form of a coherent precipitate to reduce strain energy. To evaluate this effect, values of lattice-parameter mismatch, determined by subtracting matrix lattice parameter from the  $\gamma'$  lattice parameter for the longest aging time at each temperature, Table III, are related in Fig. 12 to qualitative estimates of  $\gamma'$  morphology. Particle shape designations, in order of increasing degree of cubicity, are as follows: spheroidal (the most nearly spherical), globular (still basically spherical in shape), blocky (basically cubical in shape), and cuboidal (the most nearly cubical in shape). Fig. 12 shows that particles tend to change from spheroidal to cuboidal as the lattice-parameter mismatch increases in absolute value. This is true both when the  $\gamma'$  lattice parameter is larger than that of the  $\gamma$  matrix, and when the opposite condition exists. For example, lattice-parameter mismatch is relatively close to zero for Ni-Cr-Al alloys containing no molybdenum. As molybdenum is added, however, mismatch takes on rather large negative values, and  $\gamma'$  particles change from spheroidal to cuboidal in shape. This change is shown in the electron micrographs of Figs. 13(a) and 13(b) for 9 at. pct Al alloys aged at 1700°F (927°C). Conversely, molybdenum additions to the titanium-bearing alloys lessen considerably the large degree of mismatch that exists in the molybdenum-free base alloy. This causes  $\gamma'$  particles in specimens aged at 1700°F (927°C) to change from cuboidal to spheroidal, Figs. 13(c) and 13(d). Peter *et al.*<sup>5</sup> observed a similar tendency when 4.5 wt pct (2.7 at. pct) molybdenum was added to a Ni-Cr-Al-Ti alloy and to a Ni-Cr-Co-Al-Ti alloy.

The micrographs of Fig. 13 corroborate in rather striking fashion the aforementioned observations<sup>24-26</sup> regarding the effect of lattice-parameter mismatch on particle morphology, namely, that the morphology of particles changes from spheroidal to cuboidal as lattice-parameter mismatch increases. (It may also be noted that the effects of molybdenum on increasing the quantity of  $\gamma'$ , discussed in an earlier section, are clearly evident in Fig. 13.)

In the 12 at. pct Al alloy with the greatest lattice-parameter mismatch (5 at. pct Mo), the  $\gamma'$  precipitate exhibited a dual morphology after aging at 1700°F (927°C). Cuboids predominated after aging for 3 hr, but some particles with a rod-like appearance were also present. As the particles coarsened during subsequent aging to 112 hr, the cuboidal particles continued to coalesce into particles with the rod-like appearance, so that the latter morphology predominated after 112 hr. This tendency to develop plates or rods is consistent with the large lattice parameter mismatch<sup>24-26</sup> in this alloy of high volume fraction of  $\gamma'$ . The symbol representing this aged specimen is marked by an arrow in Fig. 12, indicating that the average morphology is that of a particle with higher lattice strain than that of a cuboid.

The fact that the minimum in the data band in Fig. 12 occurs at a mismatch of about 0.005Å instead of at zero mismatch is believed to result primarily from a difference in coefficients of thermal expansion between matrix and  $\gamma'$ . Morrow<sup>27</sup> has recently estimated that

the mean coefficient of linear thermal expansion between room temperature and 1472°F (800°C) of the  $\gamma$  matrix in the same Ni-Cr-Al alloys described in the present investigation is  $17 \times 10^{-6}/^{\circ}\text{C}$ . This is considerably higher than the value for Ni<sub>3</sub>Al in the same temperature interval,  $15 \times 10^{-6}/^{\circ}\text{C}$ , obtained by Taylor and Floyd<sup>11</sup> and by Stoeckinger and Neumann.<sup>29</sup> This difference indicates that the algebraic value of the lattice-parameter mismatch ( $a_{\gamma'} - a_{\gamma}$ ) for a specimen should increase as the specimen is cooled from the aging temperature to room temperature (the temperature at which lattice parameters were measured). Thus, data points for the three Ni-Cr-Al alloys in Fig. 12 should be displaced to the left by about 0.005Å, to represent the mismatch at 1400°F (760°C), and by about 0.006Å, to represent the mismatch at 1700°F (927°C). The results of Morrow suggest that these displacements would be reduced somewhat by molybdenum additions to the Ni-Cr-Al system. Had it been possible, therefore, to conduct the precision lattice-parameter measurements at the actual aging temperatures, the minimum in the data band of Fig. 12 would probably occur quite close to zero mismatch.

The tendency of the data points for the specimens aged at 1700°F (927°C) to lie above those for specimens aged at 1400°F (760°C) in Fig. 12, suggests that, for a given degree of lattice-parameter mismatch, the morphology of  $\gamma'$  particles becomes more cuboidal as particle size increases. This relationship between size and morphology of Ni<sub>3</sub>Al particles has been observed by Ardell and Nicholson<sup>25</sup> and by Hornbogen and Roth.<sup>26</sup>

## CONCLUSIONS

The following conclusions can be made from the investigation of the influence of molybdenum on the  $\gamma'$  phase in wrought nickel-base superalloys. Items 2 through 5 are based on studies of specimens aged at 1400° or 1700°F (760° or 927°C).

1) Molybdenum raises the  $\gamma'$  solvus temperature markedly. The effect of molybdenum declines as the solvus temperature of the base alloy increases, and as titanium is substituted for aluminum.

2) Molybdenum increases the weight fraction of  $\gamma'$  significantly by reducing the solubility of aluminum in the  $\gamma$  matrix.

3) Molybdenum dissolves extensively in  $\gamma'$  in Ni-Cr-Al-Mo alloys. Molybdenum substitutes for chromium, but has virtually no effect on the aluminum and titanium contents of the  $\gamma'$ . The molybdenum (and chromium) contents of  $\gamma'$  are significantly reduced, however, by substitution of titanium for most of the aluminum. Molybdenum contents of  $\gamma'$  are somewhat lower in specimens aged at 1700°F (927°C) than in those aged at 1400°F (760°C).

4) The lattice parameter of extracted  $\gamma'$  is increased markedly in Ni-Cr-Al-Mo alloys and moderately in Ni-Cr-Ti-Al-Mo alloys as molybdenum content increases in each series of alloys. The  $\gamma'$  lattice parameter can be predicted rather accurately from the chemical composition of the extracted particles by means of a simple linear equation derived from published results regarding the individual effects of Al, Cr, Mo, and Ti on the lattice parameter of pure nickel. The  $\gamma'$  lattice parameters of any alloy are virtually the same for the two aging temperatures of this study; furthermore, only

very small changes in lattice parameter occur as aging time increases from 63 to 1000 hr at 1400°F (760°C) and from 3 to 112 hr at 1700°F (927°C).

5) The morphology of  $\gamma'$  particles changes from spheroidal to cuboidal as lattice-parameter mismatch increases in absolute value. This occurs with increasing molybdenum content in titanium-free alloys and with decreasing molybdenum content in the 2 at. pct Al-4 at. pct Ti alloys.

#### ACKNOWLEDGMENT

The following contributions to this research are most gratefully acknowledged: The valuable suggestions and guidance of Professor O. F. Kimball, particularly concerning lattice-parameter measurements, the constructive advice of Professors L. O. Brockway, W. A. Hosford, E. E. Huckle, W. C. Bigelow, and J. B. Newkirk and of Dr. A. Havalda and Dr. O. H. Kriege, the provocative discussions with Dr. D. J. Wilson, Dr. P. D. Goodell, and Dr. Y. E. Smith, and the invaluable assistance of Mr. V. Biss toward the electron metallographic phase of this research. The principal author is deeply indebted to the Climax Molybdenum Company of Michigan for financial support and for the use of laboratory facilities throughout the course of this study.

#### REFERENCES

1. R. W. Guard and E. A. Smith: *J. Inst. Metals*, 1959-60, vol. 88, p. 283.
2. R. W. Guard and J. H. Westbrook: *Trans TMS-AIME*, 1959, vol. 215, p. 807.

3. J. R. Mihalisin and D. L. Pasquine: Proc. of the Int. Symp. on Structural Stability in Superalloys, Seven Springs, Pa., September, 1968, p. 134.
4. O. H. Kriege and J. M. Baris: *Trans. ASM*, 1969, vol. 62, p. 195.
5. W. Peter, H. Muller, and E. Kohlhaas: *Arch. Eisenhuttentw.*, 1967, vol. 38, p. 329.
6. A. Havalda: *Trans. ASM*, 1969, vol. 62, p. 477.
7. L. R. Woodyatt, C. T. Sims, and H. J. Beattie, Jr.: *Trans. TMS-AIME*, 1966, vol. 236, p. 519.
8. W. T. Loomis: Ph.D. Thesis, University of Michigan, 1969.
9. R. W. Floyd: *J. Inst. Metals*, 1951-52, vol. 80, p. 551.
10. A. Taylor and R. W. Floyd: *J. Inst. Metals*, 1952-53, vol. 81, p. 451.
11. A. Taylor and R. W. Floyd: *J. Inst. Metals*, 1952-53, vol. 81, p. 25.
12. A. Taylor and R. W. Floyd: *J. Inst. Metals*, 1951-52, vol. 80, p. 577.
13. A. Taylor: *Trans. AIME*, 1956, vol. 206, p. 1356.
14. D. L. Sponseller: Climax Molybdenum Company of Michigan, Ann Arbor, Michigan, unpublished research, 1971.
15. O. H. Kriege and C. P. Sullivan: *Trans. ASM*, 1968, vol. 61, p. 278.
16. V. Biss: Climax Molybdenum Company of Michigan, Ann Arbor, Michigan, unpublished research, 1971.
17. D. H. Maxwell: *ASM Metals Eng. Quart.*, November 1970, p. 42.
18. R. L. Dreshfield and R. L. Ashbrook: *NASA TN-D-6015*, September, 1970.
19. R. F. Decker and C. G. Bieber: *Symp. on Electron Metallography*, ASTM Spec. Tech. Publ. No. 262, 1960, p. 120.
20. J. S. Slaney: Proc. of the Int. Symp. on Structural Stability in Superalloys, Seven Springs, Pa., September 1968, p. 67.
21. G. N. Maniar and J. E. Bridge, Jr.: *Met. Trans.*, 1971, vol. 2, p. 95.
22. R. Nordheim and N. J. Grant: *Trans. AIME*, 1954, vol. 200, p. 211.
23. W. B. Pearson: *Lattice Spacings and Structures of Metals and Alloys*, Pergamon Press, New York, 1958.
24. W. C. Hagel and H. J. Beattie, Jr.: *Precipitation Processes in Steels*, Spec. Rep. No. 64, Iron and Steel Inst., 1959, p. 98.
25. A. J. Ardell and R. B. Nicholson: *Acta Met.*, 1966, vol. 14, p. 1295.
26. E. Hornbogen and M. Roth: *Z. Metallk.*, 1967, vol. 58, p. 842.
27. H. Morrow III: Climax Molybdenum Company of Michigan, Ann Arbor, Mich., unpublished research, 1971.
28. G. R. Stoekinger and J. P. Neumann: *J. Appl. Cryst.*, 1970, vol. 3, p. 32.